

DNA Sequence Context as a Determinant of the Quantity and Chemistry of Guanine Oxidation Produced by Hydroxyl Radicals and One-electron Oxidants*^[5]

Received for publication, September 3, 2008, and in revised form, October 10, 2008. Published, JBC Papers in Press, October 23, 2008, DOI 10.1074/jbc.M806809200

Yelena Margolin^{†1}, Vladimir Shafirovich[§], Nicholas E. Geacintov[§], Michael S. DeMott[‡], and Peter C. Dedon^{‡2}

From the [‡]Department of Biological Engineering and Center for Environmental Health Sciences, Massachusetts Institute of Technology, Cambridge, Massachusetts 02139 and the [§]Department of Chemistry and Radiation and Solid State Laboratory, New York University, New York, New York 10003

DNA sequence context has emerged as a critical determinant of the location and quantity of nucleobase damage caused by many oxidizing agents. However, the complexity of nucleobase and 2-deoxyribose damage caused by strong oxidants such as ionizing radiation and the Fenton chemistry of Fe²⁺-EDTA/H₂O₂ poses a challenge to defining the location of nucleobase damage and the effects of sequence context on damage chemistry in DNA. To address this problem, we developed a gel-based method that allows quantification of nucleobase damage in oxidized DNA by exploiting *Escherichia coli* exonuclease III to remove fragments containing direct strand breaks and abasic sites. The rigor of the method was verified in studies of guanine oxidation by photooxidized riboflavin and nitrosoperoxycarbonate, for which different effects of sequence context have been demonstrated by other approaches (Margolin, Y., Cloutier, J. F., Shafirovich, V., Geacintov, N. E., and Dedon, P. C. (2006) *Nat. Chem. Biol.* 2, 365–366). Using duplex oligodeoxynucleotides containing all possible three-nucleotide sequence contexts for guanine, the method was used to assess the role of DNA sequence context in hydroxyl radical-induced guanine oxidation associated with γ -radiation and Fe²⁺-EDTA/H₂O₂. The results revealed both differences and similarities for G oxidation by hydroxyl radicals and by one-electron oxidation by riboflavin-mediated photooxidation, which is consistent with the predominance of oxidation pathways for hydroxyl radicals other than one-electron oxidation to form guanine radical cations. Although the relative quantities of G oxidation produced by hydroxyl radicals were more weakly correlated with sequence-specific ionization potential than G oxidation produced by riboflavin, damage produced by both hydroxyl radical generators and riboflavin within two- and three-base runs of G showed biases in location that are consistent with a role for electron transfer in defining the location of the damage products. Furthermore, both γ -radiation and Fe²⁺-EDTA/H₂O₂ showed rel-

atively modest effects of sequence context on the proportions of different damage products sensitive to *E. coli* formamidopyrimidine DNA glycosylase and hot piperidine, although GT-containing sequence contexts displayed subtle biases in damage chemistry (formamidopyrimidine DNA glycosylase/piperidine ratio). Overall, the results are consistent with the known chemistry of guanine oxidation by hydroxyl radical and demonstrate that charge migration plays a relatively minor role in determining the location and chemistry of hydroxyl radical-mediated oxidative damage to guanine in DNA.

With implications for mutagenesis and carcinogenesis, DNA damage caused by strong oxidizing agents such as ionizing radiation and Fenton chemistry (e.g. Fe²⁺-EDTA, Cu⁺/H₂O₂) affects both the base and sugar moieties (1, 2). This complexity poses a challenge to understanding the mechanisms of formation of the ultimate stable oxidation products and their relative amounts, especially in terms of defining the effects of DNA sequence context on the quantity and location of the damage. For example, ionizing radiation causes DNA damage by oxidation through both “direct” (non-scavengeable) and “indirect” (scavengeable) pathways, in roughly equal proportions that affect both the base and 2-deoxyribose components (2–4). The indirect pathway is mediated mainly by products of water radiolysis such as hydroxyl radicals that react with DNA by hydrogen atom abstraction from the 2-deoxyribose moiety to produce strand breaks and abasic sites, and by addition to nucleobases to form a variety of damage products (5–7). The direct effect of γ -radiation entails energy deposition that leads to ionization of the DNA nucleobases and the sugar-phosphate backbone, again leading to base damage and strand breaks (5).

This complicated mixture of sugar and base damage produced by strong oxidants in DNA has hampered studies of the sequence selectivity of nucleobase oxidation, which is critical for defining the contributions of charge transfer to the spectrum of DNA lesions and for quantifying influences of local DNA structure on the final spectrum of damage products. The role of charge transfer in oxidatively damaged DNA has been well characterized in model systems involving direct photooxidation reactions (8) and those mediated by agents such as pterins (9), anthraquinones (10), rhodium complexes (11), and riboflavin (12). These agents oxidize mainly DNA nucleobases

* This work was supported, in whole or in part, by National Institutes of Health Grants CA110261 (NCI) and ES002109 (NIEHS Center grant). The costs of publication of this article were defrayed in part by the payment of page charges. This article must therefore be hereby marked “advertisement” in accordance with 18 U.S.C. Section 1734 solely to indicate this fact.

^[5] The on-line version of this article (available at <http://www.jbc.org>) contains supplemental Fig. 1.

¹ Present address: Harvard Proteomics Research, Dept. of Genetics and Complex Diseases, Harvard School of Public Health, Boston, MA 02115.

² To whom correspondence should be addressed: Dept. of Biological Engineering, NE47-277, Massachusetts Institute of Technology, 77 Massachusetts Ave., Cambridge, MA 02139. Fax: 617-324-7554; E-mail: pcdedon@mit.edu.

Sequence-selective Guanine Oxidation by Hydroxyl Radicals

by a common mechanism that is presumed to involve one-electron oxidation of guanine (G) to form a guanine radical cation ($G^{\cdot+}$),³ because of the favorable redox potential for G relative to the other nucleobases (1.29 V *versus* NHE for the guanine neutral radical, $G(-H)^{\cdot}$; 1.58 V *versus* NHE for $G^{\cdot+}$; see Ref. 13). The resulting electron hole migrates through the π -stack of B-DNA in competition with trapping to form stable products (10–12), with the common observation of damage “hot spots” at sites containing multiple adjacent guanines (*e.g.* GG, GGG). *Ab initio* calculations by Saito *et al.* (12, 14) and Senthilkumar *et al.* (15) revealed sequence-specific variations in the ionization potentials (IP) of G, with the lowest guanine IPs occurring in runs of G. Saito *et al.* (12) further correlated sequence-specific IP with the reactivity of G toward riboflavin-mediated photooxidation and derived the expected inverse correlation between reactivity and IP, an observation later verified directly by photoelectron spectroscopy (8).

Similar arguments for charge migration have been made for the direct effect of ionizing radiation. Although electron gain from the direct type effects occurs mainly with the formation of cytosine and thymine anions (16–19), electron loss occurs most frequently at Gs, with $G^{\cdot+}$ being the predominant species formed with γ -radiation (13, 17, 20). However, direct type effects also produce a significant amount of ionization of the sugar-phosphate backbone (*e.g.* Refs. 21–24), with the ensuing formation of strand breaks and abasic sites comprising ~25% of the total damage (23). This high background of strand breaks complicates analysis of the sequence selectivity of base oxidation and necessitates the use of indirect approaches in studies of charge transfer with ionizing radiation, such as the use of easily ionized base analogs. For example, Doddridge *et al.* (26) demonstrated that 7,8-dihydro-8-oxoguanine (8-oxo-G), with its lower reduction potential than G (0.74 V *versus* NHE; see Ref. 25), served as a damage hot spot when placed in an oligodeoxynucleotide that was subjected to γ -irradiation under dry film conditions that obviate the indirect effects. The use of such base analogs in solution studies with ionizing radiation, however, is complicated by artifacts such as the generation of secondary radical-mediated oxidizing species from the quenching agents used to obviate the indirect effects (27).

DNA damage by strong oxidants yields a mixture of strand breaks and base damage, thereby greatly complicating sequence-specific analysis of nucleobase oxidation. To address this problem, we have developed a gel-based method that allows quantification of nucleobase damage in oxidized DNA by exploiting *Escherichia coli* exonuclease III (ExoIII) to remove fragments containing direct strand breaks and abasic sites. The rigor of the method was verified in studies of G oxidation by riboflavin-mediated photooxidation or nitrosoperoxycarbon-

ate (ONOOCO_2^-), for which dramatically different effects of sequence context have been demonstrated by other approaches (12, 28). Using γ -radiation and Fe^{2+} -EDTA, the method was applied to test the hypothesis that hydroxyl radical-induced guanine oxidation would not be affected by sequence context because of the predominance of oxidation pathways other than one-electron oxidation to form $G^{\cdot+}$ radical cations.

EXPERIMENTAL PROCEDURES

Materials—Phosphorothioate-modified oligodeoxynucleotides were purchased from Integrated DNA Technologies (Coralville, IA) and gel-purified. All other reagents and chemicals were used without further purification. [γ -³²P]ATP with activity of 6000 Ci/mmol was purchased from PerkinElmer Life Sciences. Piperidine, ferrous sulfate, riboflavin, and 30% (w/w) hydrogen peroxide solution were purchased from Sigma. All enzymes were purchased from New England Biolabs (Ipswich, MA). Chelex-100 was purchased from Bio-Rad. Potassium phosphate, sodium bicarbonate, and EDTA were purchased from VWR (West Chester, PA). Peroxynitrite solution was purchased from Cayman Chemical (Ann Arbor, MI). Distilled and deionized water was purified using a Milli-Q system from Millipore (Bedford, MA) and was used for all experiments.

Labeling and Annealing of Oligodeoxynucleotides—Purified single-stranded oligodeoxynucleotides were 5'-end-labeled with ³²P by incubation at 37 °C for 1 h in a reaction that contained 0.2 nmol of 5' ends, 0.1 mCi of [γ -³²P]ATP, and 40 units of T4 PNK in 1× PNK buffer, in a total volume of 100 μ l. Excess label was removed by gel filtration using Sephadex G-25 columns (Roche Diagnostics) that were washed four times with a volume of 300 μ l of Chelex-treated 175 mM potassium phosphate buffer (pH 7.4). For annealing reaction, a total of 0.4 nmol of unlabeled complement was added to each purified labeled oligodeoxynucleotide; the mixture was heated at 95 °C for 5 min and was then allowed to slowly cool to room temperature over the course of 2 h.

Analysis of Damage in Double-stranded Oligodeoxynucleotides—All damage analyses and controls were performed in three separate experiments. Each Fenton reaction contained 2 mM hydrogen peroxide (concentration determined using an extinction coefficient of 39.4 $\text{M}^{-1} \text{cm}^{-1}$), 20 pmol of labeled, double-stranded oligodeoxynucleotide, and 0.1 mM FeSO_4 /EDTA (in the ratio of 1:1.1, freshly prepared before each experiment), in 175 mM Chelex-treated potassium phosphate buffer (pH 7.4) and a total volume of 50 μ l. The DNA was always added last, and the controls contained potassium phosphate buffer instead of FeSO_4 /EDTA solution. The reactions were incubated at 37 °C for 2 h, after which Fenton reagent was removed by filtration through Sephadex G-25 columns. For γ -irradiation experiments, the samples containing a total of 20 pmol of labeled, double-stranded oligodeoxynucleotide in a total of 50 μ l of Chelex-treated 175 mM potassium phosphate buffer (pH 7.4) were irradiated in a ⁶⁰Co source for a total dose of 50 gray. Following treatment, the samples were incubated at ambient temperature for 20 min before purification by filtration using Sephadex G-25 columns. Studies of oligodeoxynucleotide damage by ONOOCO_2^- and riboflavin were performed according to the procedure described previously (28).

³ The abbreviations used are: $G^{\cdot+}$, guanine radical cation; NHE, normal hydrogen electrode; Ox, oxazolone, 2,2-diamino-4-[(2-deoxy- β -D-erythro-pentofuranosyl)-amino]-5(2H)-oxazolone; CO_3^- , carbonate radical anion; 8-oxo-G, 7,8-dihydro-8-oxoguanine; Fpg, *E. coli* formamidopyrimidine DNA glycosylase; ExoIII, *E. coli* exonuclease III; Fapy-G, 2,6-diamino-5-formamido-4-hydroxypyrimidine; G, guanine; $G(-H)^{\cdot}$, guanine neutral radical; 4-OH-G $^{\cdot}$, 4-hydroxyguanine neutral radical; 8-OH-G $^{\cdot}$, 8-hydroxyguanine neutral radical; IP, ionization potential; NO_2^{\cdot} , nitrogen dioxide radical; ONOOCO_2^- , nitrosoperoxycarbonate; ONOO^- , peroxyntirite.

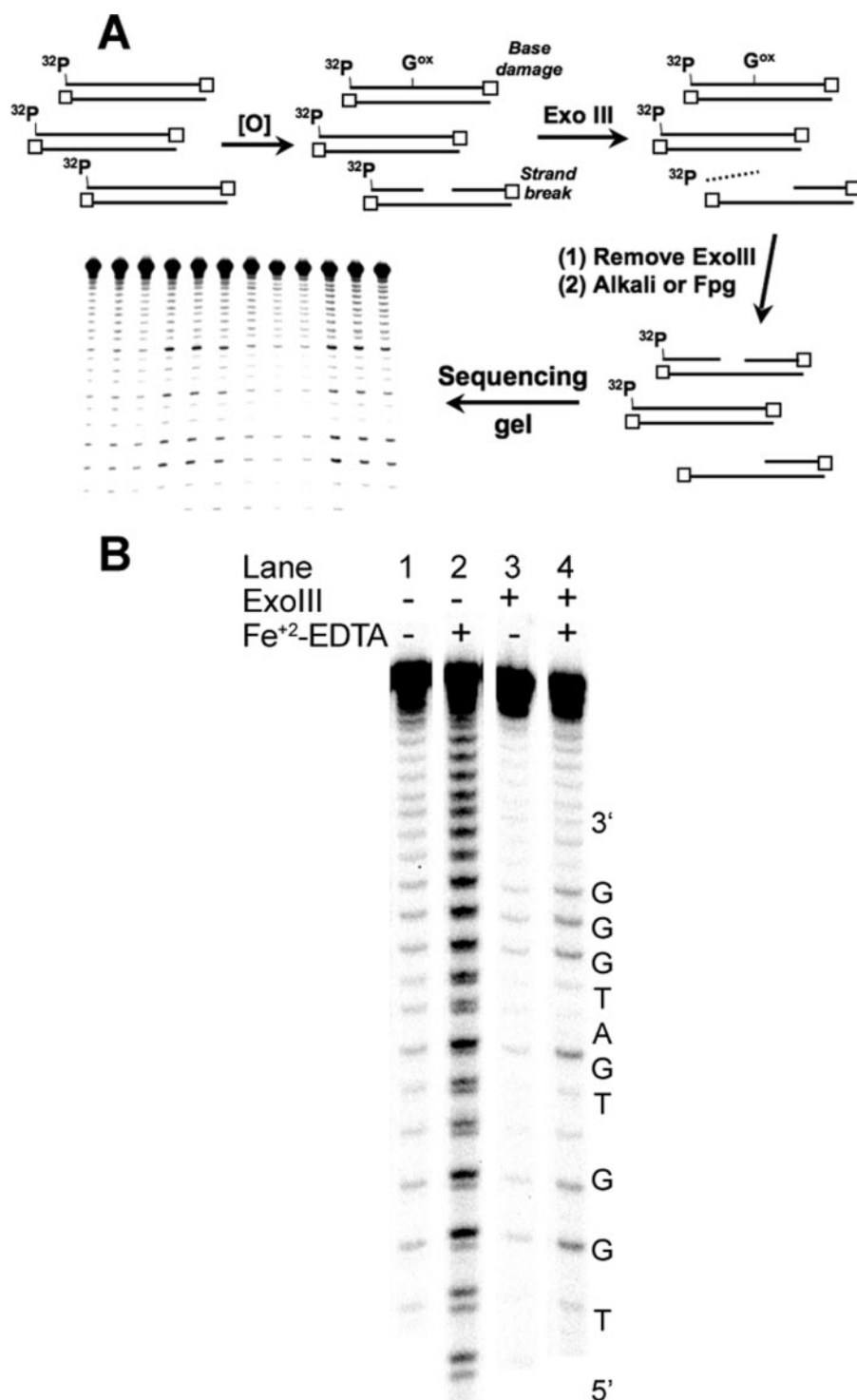


FIGURE 1. ExoIII-mediated removal of DNA containing strand breaks for sequencing gel analysis of G oxidation. *A*, schematic presentation of the ExoIII approach to strand break removal. *B*, demonstration of strand break removal with ExoIII. A ³²P-labeled double-stranded oligodeoxynucleotide (S1-S in Table 1) was treated with Fe²⁺-EDTA/H₂O₂ and subsequently with ExoIII. Base damage was converted to strand breaks by treatment with hot piperidine, and the resulting fragments were resolved by denaturing PAGE (20%) as described under "Experimental Procedures."

Damaged and purified oligodeoxynucleotides were treated with 5 units of ExoIII in 1× NE buffer 1 (New England Biolabs, Ipswich, MA) at 37 °C for 1 h in a total volume of 60 μl. These conditions were sufficient to remove all direct strand breaks generated during damage reactions, as determined by control

experiments (results not shown). For hot piperidine treatment, oligodeoxynucleotides were desalted by gel filtration, incubated with 1 M piperidine at 90 °C in a total volume of 120 μl, lyophilized, and dissolved in a total of 5 μl of formamide gel loading buffer (28). To remove ExoIII activity prior to Fpg reactions, oligodeoxynucleotides were incubated with 20 mM EDTA to chelate Mg²⁺ present in 1× NE buffer 1 and passed through protein-binding Micropure-EZ filters (Millipore, Bedford, MA). The oligodeoxynucleotides were subsequently treated with 8 units of Fpg at 37 °C for 1 h, precipitated with ethanol, and dissolved in a total of 5 μl of formamide gel loading buffer.

A total of 2 μl of each sample was resolved on a 20% polyacrylamide gel containing 8 M urea and was subjected to PhosphorImager analysis (ImageQuant, GE Healthcare). Relative reactivities of Gs in each oligodeoxynucleotide sequence were determined as described previously (28).

RESULTS

Development of an Exonuclease Digestion Method for Quantifying Nucleobase Damage in Oligodeoxynucleotides—One approach to quantifying the sequence specificity of nucleobase damage employs controlled reactions in ³²P-labeled, double-stranded oligodeoxynucleotides, with sequencing gel analysis of strand breaks formed when nucleobase lesions are expressed as strand breaks by treatment with hot alkali (e.g. piperidine) or with DNA N-glycosylase repair enzymes that recognize damaged nucleobases (e.g. *E. coli* formamidopyrimidine DNA glycosylase, Fpg) (12, 28). The major limitation of this approach is interference from direct strand breaks and labile abasic sites arising from 2-deoxyribose oxidation with agents such as γ-radiation and Fenton

chemistry that damage both the base and sugar moieties (29). To resolve this problem, we devised a method to remove interfering direct strand breaks and abasic sites and thus allow for the direct analysis of nucleobase oxidation, as illustrated in Fig. 1*A*. The method utilizes double-stranded oligodeoxynucle-

Sequence-selective Guanine Oxidation by Hydroxyl Radicals

TABLE 1

Sequences of oligodeoxynucleotides used for damage analysis

Target guanines are in boldface type, and trinucleotide motifs are underlined. The invariant TGG sequence used for normalizing the quantity of damage is italicized, and asterisks denote phosphorothioate linkages.

Oligodeoxynucleotide	Sequence (5' → 3')
S1-S	CGTACTCTT <u>TGGT</u> GATGG TTCTTTC*T*A*T
S2-S	CGTACTCTT <u>TGGT</u> CGTTC TTCTTTC*T*A*T
S3-S	CGTACTCTT <u>TGGT</u> AGTTG ATTCTTTC*T*A*T
S4-S	CGTACTCTT <u>TGGT</u> AGTTC TTCTTTC*T*A*T
S5-S	CGTACTCTT <u>TGGT</u> CGTCA TTCTTTC*T*A*T
S6-S	CGTACTCTT <u>TGGT</u> AGCTA ATTCTTTC*T*A*T
S8-S	CGTACTCTT <u>TGGT</u> CGTCC TTCTTTC*T*A*T
S12-S	CGTACTCTT <u>TGGT</u> AGCTG TTCTTTC*T*A*T

otides (Table 1) containing three consecutive phosphorothioate linkages at the 3' end of each strand to protect the strands from degradation by the 3'-to-5'-exonuclease activity of ExoIII (30, 31). Upon treatment of damaged oligodeoxynucleotides with the combined 3'-to-5'-exonuclease and AP endonuclease activities of ExoIII (30, 31), the oligodeoxynucleotides that contain abasic sites and direct strand breaks with unprotected 3' ends are degraded, and the resulting ³²P-containing small fragments are either lost during processing of the oligodeoxynucleotides or during sequencing gel electrophoresis (see supplemental Fig. 1 for a typical gel). The remaining full-length, 5'-³²P-labeled oligodeoxynucleotides are protected from ExoIII degradation by the phosphorothioates at the 3' end and are either undamaged or contain only nucleobase damage. Following inactivation (chelation of Mg²⁺ cofactor by EDTA; see Ref. 32) and removal of the enzyme by passing the reaction mixture through protein-binding filters, the nucleobase damage is converted to strand breaks by treatment with hot piperidine or Fpg. Sequencing gel analysis now reveals the location and quantity of nucleobase damage caused by the oxidizing agent, without interference from direct strand breaks or abasic sites.

Validation of the ExoIII Method—The method was validated in two ways. The first set of studies was designed to assess the effects of ExoIII digestion on the nucleobase damage produced by two oxidants, riboflavin-mediated photooxidation and ONOOCO₂⁻, that cause well defined G oxidation in terms of quantity and location and that cause few strand breaks or abasic sites (28). The studies were conducted in a series of oligodeoxynucleotides (shown in Table 1) with the following general structure: 5'-CGTACTCTTTGGTX₁G₁Y₁TX₂G₂Y₂TTCTTTC*T*A*T-3'. Each contains three consecutive phosphorothioate linkages (asterisks), two Gs in variable three-nucleotide sequence contexts (X_iG_iY_i), and an invariant TGG damage site for normalizing damage levels across all of the oligodeoxynucleotides (12, 28). Following treatment of duplex oligodeoxynucleotides with either 3 mM ONOOCO₂⁻ or 30 μM riboflavin/366 nm irradiation (28), samples were split, and one-half was treated with ExoIII for 60 min. Following inactivation and removal of ExoIII, the oligodeoxynucleotides were treated with hot piperidine, and the resulting strand breaks were quantified by sequencing gel analysis, as illustrated in Fig. 1B. The *bar graphs* shown in Fig. 2 reveal that the quantity of G oxidation detected by the sequencing gel method is not affected by ExoIII treatment, which indicates that the ExoIII digestion step did not introduce artifacts into the quantification of sequence-

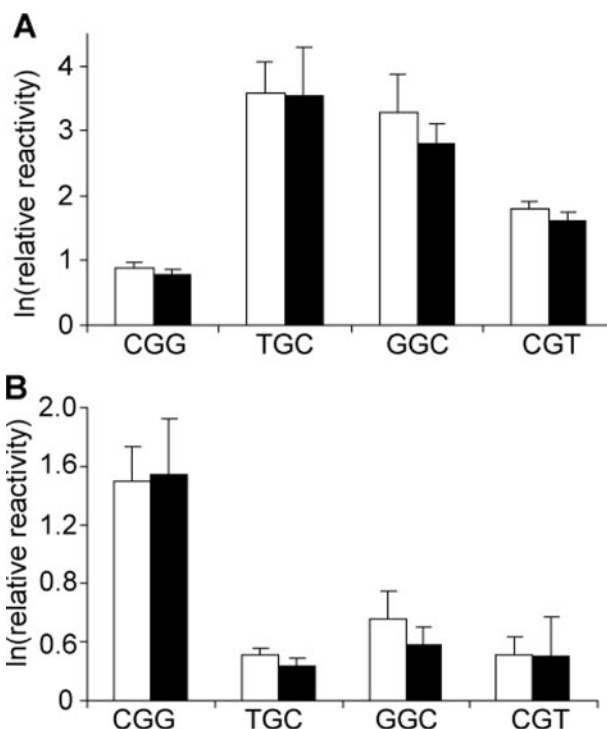


FIGURE 2. Verification of the ExoIII digestion method with sequence-selective G oxidation by ONOOCO₂⁻ and riboflavin. ³²P-labeled double-stranded oligodeoxynucleotides containing four representative G sequence contexts (Table 1) were treated with ONOOCO₂⁻ (A) or photo-activated riboflavin (B), as described under "Experimental Procedures." The sample was subsequently split, with one-half treated with ExoIII to remove direct strand breaks (*black bars*) and the other half left untreated as a control (*white bars*). Base damage in both samples was then expressed as strand breaks resulting from hot piperidine treatment, and the resulting fragments were resolved on by denaturing PAGE (20%), as described under "Experimental Procedures."

lective G oxidation in the oligodeoxynucleotides. The results are also consistent with our previous studies, in which the level of riboflavin-mediated oxidation of G varied inversely with the sequence-specific IP of the central G in a three-nucleotide context (relative G oxidation in decreasing order CGG > GGC > CGT > TGC), whereas the opposite was true for ONOOCO₂⁻ (TGC ~ GGC > CGT > CGG) (28).

A second approach to validating the ExoIII digestion method entailed characterization of G oxidation in an oligodeoxynucleotide treated with Fe²⁺-EDTA/H₂O₂, an agent well known to oxidize 2-deoxyribose to produce strand breaks and abasic sites at all positions in DNA (29, 33) and to oxidize nucleobases (7, 34). As shown in Fig. 1B, Fe²⁺-EDTA/H₂O₂ produced a significant quantity of strand breaks at all positions in the oligodeoxynucleotide (Fig. 1B, lane 2), with the doublet band pattern in the gel image arising from differential migration of oligodeoxynucleotide fragments containing 3-phosphate and 3'-phosphoglycolate ends (35, 36). Incubation of the damaged oligodeoxynucleotide with ExoIII prior to hot piperidine treatment substantially diminished the background of direct strand breaks and revealed damage mainly at Gs (Fig. 1B, lane 4). The combined results of these validation studies indicate that ExoIII is effective at removing strand breaks and oxidized abasic sites without interfering with nucleobase damage.

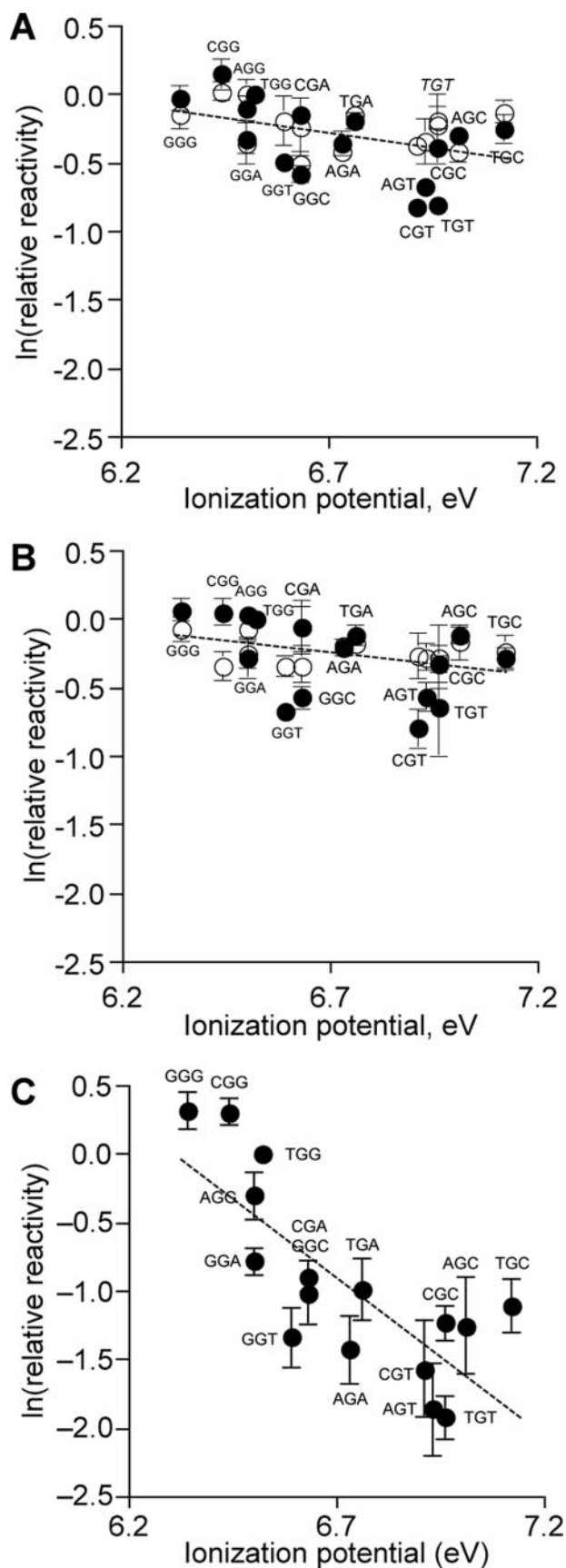


FIGURE 3. Relative reactivities of Gs in different sequence contexts as a function of their sequence-specific ionization potentials. Labeled oligodeoxynucleotides with sequences shown in Table 1 were subjected to

Assessment of the Sequence Selectivity of G Oxidation Produced by γ -Radiation and Fe^{2+} -EDTA/ H_2O_2 —The ExoIII digestion and sequencing gel method was employed to define the role of sequence context in hydroxyl radical-mediated G oxidation, with comparison to one-electron oxidation by riboflavin-mediated photooxidation. The studies were initiated by performing damage reactions with each of the ^{32}P -labeled, double-stranded oligodeoxynucleotides shown in Table 1 in 175 mM metal-free phosphate buffer at pH 7.4. Optimal doses for γ -irradiation (^{60}Co , 1.1 gray/min) and Fe^{2+} -EDTA/ H_2O_2 treatment were chosen to produce a range of quantifiable damage signals from the sequencing gels and to cause a maximum of one detectable base oxidation event per oligodeoxynucleotide molecule, which, according to a Poisson distribution, occurs when less than 30% of the parent duplex is consumed following removal of strand breaks by ExoIII treatment and base damage expression by hot piperidine or Fpg. In light of the uncertainty about the exact nature of iron-based Fenton chemistry (37), we chose reaction conditions that would maximize hydroxyl radical production in an air-saturated solution as follows: 0.1 mM Fe^{2+} -EDTA, 2 mM H_2O_2 in 175 mM Chelex-treated potassium phosphate buffer (pH 7.4) for 2 h at 37 °C (37).

As shown in Fig. 3 for piperidine-labile G damage products, the reactivity at each G was determined relative to the central G of the TGG normalization sequence contained in each oligodeoxynucleotide (Table 1). The $\ln(\text{relative reactivity})$ data were plotted as a function of the sequence-specific IP of the G (*open circles* in Fig. 3; see supplemental Fig. 1 for a typical gel used for quantification). In the case of XGG, GGX, and GGG sequences, the relative damage level was determined for the central G to be consistent with our previous studies of G oxidation by photooxidized riboflavin and ONOOCO_2^- (28). For both γ -radiation and Fe^{2+} -EDTA/ H_2O_2 , the $\ln(\text{relative activity})$ of G varied only modestly with sequence context, within a range of 0.60–1.0 for γ -radiation and 0.71–0.96 for Fe^{2+} -EDTA/ H_2O_2 . Similar trends were observed with Fpg-labile G oxidation for both agents (*closed circles* in Fig. 3; see supplemental Fig. 1), although relatively lower reactivity was observed for 5'-CGT-3', 5'-AGT-3', 5'-TGT-3', 5'-GGT-3', and 5'-GGC-3' (0.4–0.6 for γ -radiation and 0.5–0.6 for Fe^{2+} -EDTA).

Assessment of the Sequence Selectivity of G Oxidation Produced by γ -Radiation and Fe^{2+} -EDTA/ H_2O_2 within Runs of G—In addition to the correlation between IP and sequence context-dependent G reactivity as evidence of charge transfer,

oxidation by 50 gray of γ -irradiation (A), 0.1 mM Fe^{2+} -EDTA/2 mM H_2O_2 (B), and riboflavin-mediated photooxidation (C). Subsequent to treatment with ExoIII to remove the background of 2-deoxyribose oxidation, the oligodeoxynucleotides were treated with hot piperidine (○) or Fpg (●) to convert oxidized bases to strand breaks and subjected to sequencing gel electrophoresis. For all three oxidants, the relative reactivity of each G was calculated as the percentage of total radioactivity in the corresponding band, relative to the damage induced within the central G of the invariant TGG sequence, quantified after autoradiography as described under “Experimental Procedures.” Data for riboflavin-mediated photooxidation were taken from Margolin *et al.* (28). Data in all three panels were plotted on the same y axis scale for purposes of comparison and represent the mean \pm S.D. for three experiments. Dashed lines represent linear regression fits of combined piperidine and Fpg data for γ -irradiation ($y = -0.469x + 2.88$; $r^2 = 0.22$) and Fe^{2+} -EDTA/2 mM H_2O_2 ($y = -0.376x + 2.28$; $r^2 = 0.16$) and of riboflavin-mediated photooxidation data from Margolin *et al.* (28) ($y = -2.30x + 14.5$; $r^2 = 0.61$); all lines have statistically significant negative slopes, as noted in the text.

Sequence-selective Guanine Oxidation by Hydroxyl Radicals

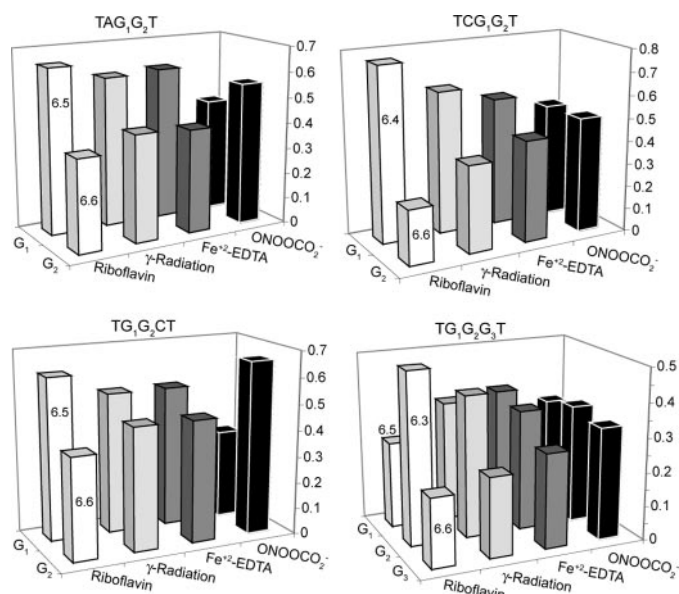


FIGURE 4. Relative oxidative damage sustained by individual Gs within four representative G runs for four oxidizing agents. Numbers on the columns for riboflavin-mediated photooxidation correspond to the sequence-specific calculated ionization potential (eV) for each G identified in the sequence above each graph and along the z axis (12). The y axis corresponds to the fraction of the total γ -radiation-induced oxidative damage sustained by all Gs in the run of Gs. The data represent the mean for three experiments; the standard deviation for all of the data is <10%.

G oxidation by classical one-electron oxidants such as photoactivated riboflavin has also been observed to localize at the 5'-most G in GG motifs, and variably at the 5'- or middle G of GGG (38), as a result of charge transfer. Although the sequence context studies revealed no significant preference for damage in runs of G by γ -radiation or Fe^{2+} -EDTA/ H_2O_2 compared with other sequence contexts (Fig. 3), we sought to determine whether the hydroxyl radical was site-selective within GG and GGG motifs. This was accomplished by quantifying the relative amount of damage sustained by G in four representative 5'-TXGXT-3' sequence contexts as a result of exposure to γ -radiation and Fe^{2+} -EDTA/ H_2O_2 , with the relative reactivity expressed as the fraction of total G oxidation in a pair or trio of Gs. As shown in Fig. 4, the quantity of damage produced by photooxidized riboflavin exhibits an inverse correlation with the calculated G IP values, which is consistent with the previous studies of Saito and co-workers (12, 14), most notably for the TGGGT sequence context (38). The results with ONOOCO_2^- reveal a weaker dependence on the IP of G, as shown in Fig. 4 and in our previously published studies (28). In the case of the $\text{TG}_1\text{G}_2\text{CT}$ sequence, ONOOCO_2^- was highly selective for the G2 position adjacent to C, which is consistent with the direct relationship between G IP and reactivity observed for ONOOCO_2^- (28). The results with γ -radiation and Fe^{2+} -EDTA/ H_2O_2 indicate that oxidation is slightly favored at the 5'-G in GG sequence contexts except in $\text{TG}_1\text{G}_2\text{G}_3\text{T}$, where there G₂ and G₁ sustain similar levels of damage. These results are similar to the riboflavin data, with less pronounced selectivity.

Estimation of the Sequence Dependence of G Oxidation Chemistry Caused by γ -Radiation and Fe^{2+} -EDTA/ H_2O_2 —In addition to the effects on the quantity of G oxidation, sequence context may also affect the chemistry of the damage. One

approach to assessing the sequence dependence of G oxidation chemistry entails quantification of the differential sensitivity of the lesions to hot piperidine and Fpg treatments. It is well established that the reactivity of different G oxidation products with piperidine and Fpg is variable and depends upon the structures of the lesions (39) with 8-oxo-dG and the 2,6-diamino-5-formamido-4-hydroxypyrimidine form of dG (Fapy-dG) sensitive to Fpg and resistant to piperidine treatment (39–42). The opposite is true for the G oxidation product 2,2-diamino-4-[(2-deoxy- β -D-erythro-pentofuranosyl)-amino]-5(2H)-oxazolone (oxazolone; Ox), the stable degradation product of the 2-aminoimidazolone lesion (39, 43, 44). The diastereomeric spiroimidodihydroantoin lesions, a major product of G oxidation by carbonate radical anion ($\text{CO}_3^{\cdot-}$) in DNA (45) and a minor product of 8-oxo-dG oxidation in riboflavin-mediated photooxidation (46), are Fpg-sensitive but only partially alkali-labile (47). Because the major G oxidation products arising from γ -irradiation of DNA include, among a minority of other products, the Fpg-sensitive Fapy-dG and 8-oxo-dG and the piperidine-sensitive Ox (48, 49), we set out to estimate the sequence specificity of G oxidation chemistry using the approach of Spassky and Angelov (39) by measuring differences in the proportions of Fpg- and piperidine-sensitive lesions in the various sequence contexts.

As shown in Fig. 5, the ratios of Fpg- to piperidine-sensitive lesions produced by γ -radiation and Fe^{2+} -EDTA/ H_2O_2 in all sequence contexts vary over an ~ 2 -fold range. This range of ratios is similar to that observed with riboflavin-mediated photooxidation (Fig. 5), but it stands in contrast to the 5.5-fold variation in the ratios of Fpg- to piperidine-sensitive lesions produced by ONOOCO_2^- (28). As noted earlier, Gs within 5'-GT-3' motifs (5'-CGT-3', 5'-AGT-3', 5'-GGT-3', and 5'-TGT-3') are characterized by Fpg/piperidine ratios that are significantly lower than the other ratios ($p < 0.02$) and range from 0.5 to 0.7 for γ -radiation and from 0.6 to 0.8 for Fe^{2+} -EDTA/ H_2O_2 . In addition, the 5'-GGC-3' sequence context is also characterized by a relatively low Fpg/piperidine ratio of 0.8 in the case of damage produced by Fe^{2+} -EDTA/ H_2O_2 .

DISCUSSION

The complexity of nucleobase and sugar damage caused by strong oxidizing agents such as ionizing radiation and the Fenton chemistry typified by Fe^{2+} -EDTA/ H_2O_2 poses a challenge to defining the location of nucleobase damage and the effects of sequence context on the damage. To address this problem, we developed a gel-based method that allows quantification of nucleobase damage in oxidized DNA by exploiting ExoIII to remove fragments containing direct strand breaks and abasic sites. The feasibility of this approach was proven in two sets of studies. The first entailed corroboration of the sequence selectivity of G oxidation by riboflavin-mediated photooxidation and by ONOOCO_2^- (Fig. 2). These agents were previously observed to cause G oxidation with widely differing sequence selectivity; the level of riboflavin-mediated oxidation of G decreases as a function of the sequence-specific IP of the central G in a three-nucleotide context (relative G oxidation in decreasing order $\text{CGG} > \text{GGC} > \text{CGT} > \text{TGC}$), whereas the opposite is true for ONOOCO_2^- ($\text{TGC} \sim \text{GGC} > \text{CGT} > \text{CGG}$)

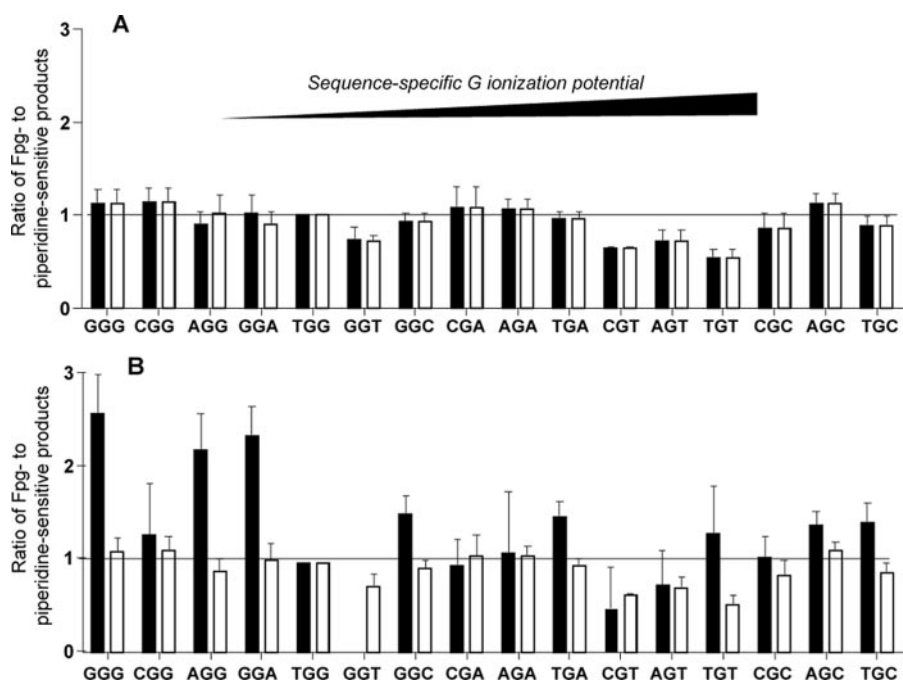


FIGURE 5. Ratios of relative amounts of Fpg- to piperidine-sensitive oxidized G lesions produced by Fe^{2+} -EDTA/ H_2O_2 (white bars) and γ -radiation (black bars) (A) and riboflavin-mediated photooxidation (white bars) and ONOOCO_2^- (black bars; data from Ref. 28) within different sequence contexts (B). Values represent mean \pm S.D. for three experiments. The sequence contexts are organized from left to right as a function of increasing IP.

(28). This behavior is identical to that observed in studies employing ExoIII (Fig. 2). Furthermore, ExoIII digestion of oligodeoxynucleotides treated with Fe^{2+} -EDTA/ H_2O_2 caused a significant reduction in the direct strand breaks and abasic sites produced by this agent, with the remaining damage confined to G bases (Fig. 1B), as expected from previous studies (7, 34).

The ExoIII approach to removing strand breaks and abasic sites can be used to probe sequence selectivity of nucleobase oxidation by other oxidants that generate substantial amounts of 2-deoxyribose oxidation, such as ionizing radiation, peroxynitrite (ONOO^-) (44), and peroxy radicals (50). Previous approaches to studying nucleobase oxidation in Fenton reactions induced by Cu^+ and Fe^{2+} in the presence of H_2O_2 and ascorbate addressed the strand break problem by adding sucrose to the damage reactions to suppress 2-deoxyribose oxidation (51). However, this approach generates sucrose-derived radical species that could lead to alterations of G oxidation chemistry (52).

The method was applied to define the role of sequence context in G oxidation by hydroxyl radicals, with γ -radiation and Fe^{2+} -EDTA/ H_2O_2 as model hydroxyl radical-generating systems. Both of these oxidizing agents produce a substantial quantity of 2-deoxyribose oxidation in DNA (2, 33), which would otherwise confound a gel-based analysis of G oxidation by adding 2-deoxyribose-derived strand breaks to those derived from nucleobase damage. Although nucleobase oxidation mediated by the direct effect of γ -radiation is associated with charge transfer as a result of the formation of G^+ radicals (13, 17, 20), the relatively dilute DNA concentration employed in the present studies leads to a predominance of hydroxyl radicals (*i.e.* the indirect effect) as the main DNA-damaging species

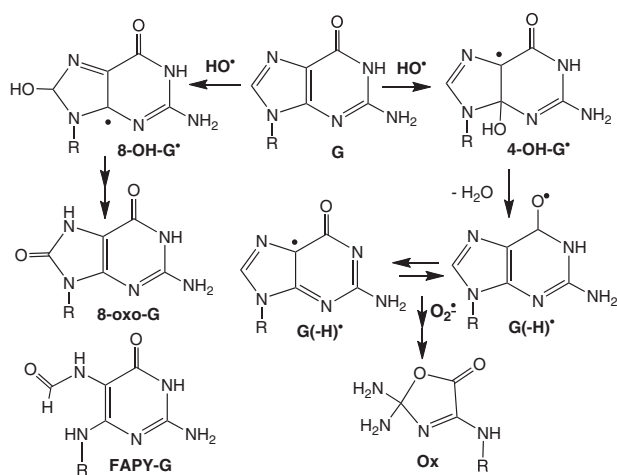
generated during γ -irradiation. In conducting these experiments, we were mindful of the proposed formation of oxidizing species other than the hydroxyl radical by the Fe^{2+} -EDTA complex (53–55), specifically oxidizing iron-oxo complexes such as the perferryl ($[\text{Fe}^{2+} - \text{O}_2 \leftrightarrow \text{Fe}^{3+} - \text{O}_2^-]$) and ferryl ($[\text{Fe}^{4+} = \text{O}]$) species (37). Although these species are strong oxidants, they are less reactive than hydroxyl radical with molecules such as benzoate, *tert*-butyl alcohol, acetate ion, arginine, and serine (53, 54), presumably because of their lower reduction potentials relative to that of hydroxyl radical (56). It has been observed that the relative yields of hydroxyl radical and the iron-oxo complexes are strongly dependent on factors such as pH, solvent polarity, buffer components, and the metal chelator (55, 57, 58). The concentration of H_2O_2 in the reaction mixture was shown to have a significant effect on the efficiency of $\cdot\text{OH}$

generation, with low concentrations ($\leq \mu\text{M}$) favoring iron-oxo species and high concentrations (mM) favoring hydroxyl radical (37, 57, 58). Taking into account the complicated chemistry of Fe^{2+} -EDTA, we conducted Fe^{2+} -EDTA-mediated DNA oxidation reactions in the presence of 2 mM H_2O_2 , which leads to predominant formation of hydroxyl radical (37).

As shown in Figs. 3–5, the G oxidation patterns observed for γ -radiation and Fe^{2+} -EDTA/ H_2O_2 showed strong similarities for the two agents, as expected for the predominant role of hydroxyl radicals in their mechanisms of DNA oxidation (2, 33, 37). However, there were differences from the one-electron oxidation mediated by photoactivated riboflavin, which is presumed to be dominated by G^+ radicals (13, 17, 20). Linear regression analysis revealed a much weaker correlation ($r^2 = 0.2$) between the level of G oxidation and the sequence-specific G IP for γ -radiation and Fe^{2+} -EDTA/ H_2O_2 (Fig. 3, A and B) compared with the stronger correlation observed for riboflavin here (Fig. 3C, $r^2 = 0.6$) and in previous studies (12, 28). However, the analysis confirmed statistically significant negative slopes for the plots shown in Fig. 3 for both hydroxyl radical generating agents and riboflavin ($p < 0.02$ and < 0.0004 , respectively), which is consistent with a weak negative correlation between IP and G reactivity.

A stronger similarity of the behavior of hydroxyl radicals and riboflavin in terms of sequence-selective G oxidation was apparent in the observed biases in damage location within GG and GGG motifs. In general, the relationship between the level of G oxidation produced by hydroxyl radicals and the calculated IP of G in the four GG- and GGG-containing sequences was less pronounced than that associated with riboflavin, but an inverse correlation between reactivity and IP is still apparent (Fig. 4).

Sequence-selective Guanine Oxidation by Hydroxyl Radicals



SCHEME 1. Hydroxyl radical-mediated guanine oxidation (6, 59).

This behavior stands in contrast to the varying pattern of G oxidation in GG and GGG sequences by ONOOCO_2^- (Fig. 4).

These observed effects of sequence context on hydroxyl radical-induced G oxidation raise questions about the basis for both the similarities and the differences with respect to one-electron oxidants such as riboflavin. The most obvious difference involves the initial step in G oxidation, with addition of the hydroxyl radical to C4 or C8 of G to produce 8-hydroxy- and 4-hydroxy-G radical species (8-OH-G \cdot and 4-OH-G \cdot ; Scheme 1) (59) as opposed to one-electron removal from G to produce G \cdot^+ with riboflavin-mediated photooxidation. The additional complication of 2-deoxyribose oxidation by hydroxyl radicals will be discussed shortly. The reactions subsequent to the initial electron removal by photoactivated riboflavin fit a widely accepted general model of charge transfer mediated by the G \cdot^+ radical, with migration of the hole to sequence contexts that confer the lowest IP to G (Fig. 3). Furthermore, the reactions of riboflavin-mediated G \cdot^+ within runs of G (e.g. GG and GGG contexts) have been explained by a more complicated model to account for differences observed with longer range sequence contexts, such as TGGG *versus* CGGG (38).

The mechanistic basis for the observed sequence context effects of hydroxyl radical-induced G oxidation is not as well defined as in the case of riboflavin-mediated photooxidation. This can be accounted for by the following considerations. As opposed to the predominance of G \cdot^+ as the initial product of one-electron oxidation of G, hydroxyl radical reacts to form 8-OH-G \cdot and 4-OH-G \cdot radicals. The subsequent transformations of 8-OH-G \cdot yield the stable products 8-oxo-G and Fapy-G (60). The loss of a water molecule from 4-OH-G \cdot at physiological pH results in G(-H) \cdot (59) that appears to undergo conversion mainly to the stable damage product Ox (61) (Scheme 1). The complicating factor here is the balance between the fates of 8-OH-G \cdot , 4-OH-G \cdot , and G(-H) \cdot . A bias toward 8-OH-G \cdot would lead to a predominance of stable damage products (i.e. 8-oxo-G and Fapy-G) formed at the initial site of G oxidation, whereas higher proportions of 4-OH-G \cdot and its dehydration product G(-H) \cdot could lead to migration of the radical to neighboring G bases, as discussed shortly. This may explain the diminished sequence context

effects on hydroxyl radical-mediated G oxidation relative to that of riboflavin.

This weak sequence dependence may arise from contributions of the G(-H) \cdot radical. It is well established that this species can arise from both dehydration of 4-OH-G \cdot and from deprotonation of G \cdot^+ , so it represents a common intermediate for G oxidation caused by riboflavin and hydroxyl radicals (62). This does not explain, however, the role of G(-H) \cdot in determining the location of the final damage products in runs of two or three Gs. At one extreme, G(-H) \cdot could simply represent an intermediate on the path to final damage products, with the sequence selectivity for damage products determined by the stability of the G(-H) \cdot radical (38). In this case, G(-H) \cdot does not participate in electron transfer reactions with neighboring bases and is consumed by reactions such as recombination with superoxide and the subsequent formation of species such as Ox (Scheme 1) (61) at the site of initial G oxidation. According to this model, the predominance of 8-OH-G \cdot , 4-OH-G \cdot , and G(-H) \cdot in the case of γ -radiation and Fe^{2+} -EDTA/ H_2O_2 treatment would explain the less pronounced sequence specificity of G oxidation product formation (Fig. 3, A and B) if hydroxyl radicals are relatively unselective in their initial oxidation of Gs at different sites in DNA. Tullius and co-workers (36) have demonstrated that the reactivities of hydroxyl radicals at different positions in 2-deoxyribose are governed in part by the solvent exposure of the hydrogen atoms at these positions, which would suggest some degree of "selectivity" of hydroxyl radical reactivities for solvent-exposed Gs as well. This may explain the weak sequence dependence of hydroxyl radical-induced G oxidation (Fig. 3, A and B) that is significantly less pronounced than the strong charge transfer-mediated sequence dependence for the distribution of final damage products with one-electron oxidants such as riboflavin (Fig. 3C) (12, 28).

The G(-H) \cdot may also participate in electron transfer in DNA. The deprotonation of the G \cdot^+ cation in DNA in solution occurs with a rate constant of $\geq 3 \times 10^6 \text{ s}^{-1}$ (63), suggesting that intra-strand proton-coupled hole transfer can occur between G(-H) \cdot and a neighboring G in DNA on slower time scales (64). G(-H) \cdot is a relatively strong oxidant, only 0.29 V weaker than G \cdot^+ (1.29 and 1.58 V *versus* NHE, respectively; see Ref. 13), so it is reasonable to assume that it can remove an electron from a neighboring G, albeit with a slower rate than G \cdot^+ because of this energy difference. This would explain the similarities between the hydroxyl radical generators and riboflavin-mediated photooxidation in terms of relative reactivity between different G sequence contexts (Fig. 3) and within runs of G (Fig. 4). Just as with G \cdot^+ , the most probable position of the G(-H) \cdot (i.e. the most stable position) determines the eventual final location of damage products in a run of Gs. This is consistent with the studies of Saito and co-workers (38), who correlated *ab initio* molecular orbital calculations with damage product analysis and concluded that the predominance of damage at the G $_2$ of TG $_1$ G $_2$ G $_3$ correlates well with the greater stability of the G(-H) \cdot at G $_2$.

Although there are similarities between the hydroxyl radical generators and the one-electron oxidant, there are clear differences. One factor possibly contributing to these differences is the oxidation of the 2-deoxyribose moiety by hydroxyl radical

but not by one-electron oxidants such as riboflavin. It is well known that hydroxyl radicals cause hydrogen atom abstraction from the 2-deoxyribose in DNA, with the resulting carbon-centered radicals capable of reacting with the C8 of purines (65, 66) and with molecular oxygen to form peroxy radicals and a host of degradation products (29, 67). Although the ExoIII digestion removes the final strand break and abasic site products of the sugar radical species, the sugar radicals could confound the mechanism of base oxidation by reacting with neighboring nucleobases to generate base radical species. Precedent for this activity comes from the observations of 5',8-cyclopurine nucleotides arising from addition of a 5'-radical at the C8 position of purines (65, 66).

In addition to the weak sequence dependence of hydroxyl radical-mediated G oxidation, we also observed limited sequence effects on the chemistry of the G damage (Fig. 5). The ratio of the quantity of Fpg-sensitive to hot piperidine-sensitive lesions has been shown to be an accurate estimate of site-specific guanine oxidation chemistry (28, 39). Indeed, the higher Fpg-to-piperidine ratios that were observed with riboflavin (Fig. 5) are consistent with the higher proportion of Fpg-sensitive lesions associated with riboflavin compared with γ -radiation (68). The major lesions observed to date with riboflavin consist of Fpg-sensitive 8-oxo-G and piperidine-sensitive Ox (39, 40, 68–70), along with smaller amounts of spiroiminodihydroantoin, which is sensitive to Fpg (46, 71) and partially labile in piperidine (47). The major stable G oxidation products in hydroxyl radical-induced DNA damage (7, 72, 73) include 8-oxo-G and Ox, along with Fapy-G, which is sensitive to both Fpg and piperidine (40). The \sim 2-fold sequence-dependent variation in the proportions of Fpg- and piperidine-sensitive lesions produced by the hydroxyl radical generators and riboflavin is smaller than the \sim 5-fold range for ONOOCO_2^- -induced G oxidation (28) and points to the modest role of sequence context in determining the spectrum of G damage products. The stronger sequence dependence of G oxidation chemistry by ONOOCO_2^- may reflect the more complicated set of reactive intermediates arising from this agent as follows: CO_3 and nitrogen dioxide radical (NO_2) (74). These studies with sequence-dependent variation in Fpg- and piperidine-sensitive G oxidation products provide testable models for analysis of damaged spectra by chemically specific methods such as mass spectrometry.

As noted earlier, the results with the 5'-GT-3' contexts present a special case of context-dependent G oxidation chemistry. The XGT sequence motifs are consistently characterized by the lowest Fpg-to-piperidine ratios for γ -radiation and Fe^{2+} -EDTA/ H_2O_2 , as well as riboflavin and ONOOCO_2^- (Fig. 5). This phenomenon is not general to Gs positioned next to pyrimidines since XGC motifs show Fpg-to-piperidine ratios similar to other sequence contexts (Fig. 5). There are many possible explanations for the unusual behavior of the XGT sequences. One involves the propensity for hydroxyl radical-mediated formation of tandem lesions at GT sequences involving both 8-oxo-G and a thymine-derived formyl residue (49, 75, 76). The tandem lesions appear to arise by attack of a thymine peroxy radical at the C8 of G (49). However, any model must also account for the fact that the unusual Fpg-to-piperidine ratios

are also observed with ONOOCO_2^- and riboflavin-mediated photooxidation. Based on the ratio of Fpg and piperidine sensitivities, the XGT context effects suggest the existence of a local structure that is unfavorable to formation of 8-oxo-G (piperidine resistance) or favorable to formation of Ox (Fpg-resistant; Fapy-G is sensitive to both Fpg and piperidine). The established intrinsic flexibility of DNA sequences containing alternating purine and pyrimidine bases (77) may favor a backbone conformation that promotes addition of the hydroxyl radical to the C4 position of G and produces a greater number of Ox lesions at the expense of 8-oxo-G. This shift to a greater proportion of piperidine-sensitive lesions is also consistent with a model of local helical instability proposed by Spassky and Angelov (39) to explain differential Fpg and piperidine sensitivities of G oxidation products. The results with the Fpg and piperidine sensitivity warrant further study to identify the spectrum of G oxidation products and the role of sequence context in defining the damage spectrum for both hydroxyl radicals and one-electron oxidants.

The observations made with ionizing radiation and Fe^{2+} -EDTA/ H_2O_2 have implications for the biological impact of G oxidation and DNA damage in general. For example, each of the various G oxidation products has a different mutagenic potential in terms of both the type of mutation and the frequency (78). This is further complicated by the recognized role of sequence context as a determinant of polymerase fidelity not only in copying normal DNA but also in translesion synthesis (79). Sequence-dependent variation in the spectrum of DNA oxidation products may thus influence the spectrum of mutations arising in oxidatively stressed cells.

In conclusion, we have developed an approach to quantifying sequence-selective nucleobase oxidation in DNA in the presence of strand breaks and have used it to demonstrate a more limited sequence selectivity for both the quantity and chemistry of G oxidation produced by the hydroxyl radical generators γ -radiation and Fe^{2+} -EDTA/ H_2O_2 compared with the one-electron oxidants riboflavin-mediated photooxidation and ONOOCO_2^- . The results are consistent with the formation of neutral G radical species (8-HO \cdot -G, 4-HO \cdot -G, G(-H) \cdot) by hydroxyl radicals as compared with the formation of G $^+$ by one-electron oxidants, but also point to the potential for intramolecular electron transfer with G(-H) \cdot as the means to account for the correlation between G reactivity and IP in GG and GGG sequences.

REFERENCES

- Breen, A. P., and Murphy, J. A. (1995) *Free Radic. Biol. Med.* **18**, 1033–1077
- von Sonntag, C. (1987) *The Chemical Basis of Radiation Biology*, Taylor & Francis, New York
- Roots, R., and Okada, S. (1975) *Radiat. Res.* **64**, 306–320
- Jones, G. D., Boswell, T. V., Lee, J., Milligan, J. R., Ward, J. F., and Weinfeld, M. (1994) *Int. J. Radiat. Biol.* **66**, 441–445
- Becker, D., and Sevilla, M. D. (1993) *Adv. Radiat. Biol.* **17**, 121–180
- Cadet, J., Delatour, T., Douki, T., Gasparutto, D., Pouget, J. P., Ravanat, J. L., and Sauvaigo, S. (1999) *Mutat. Res.* **424**, 9–21
- Frelon, S., Douki, T., Favier, A., and Cadet, J. (2002) *J. Chem. Soc. Perkin Trans. I*, 2866–2870
- Yang, X., Wang, X. B., Vorpapel, E. R., and Wang, L. S. (2004) *Proc. Natl. Acad. Sci. U. S. A.* **101**, 17588–17592

Sequence-selective Guanine Oxidation by Hydroxyl Radicals

9. Ito, K., and Kawanishi, S. (1997) *Biochemistry* **36**, 1774–1781
10. Henderson, P. T., Jones, D., Hampikian, G., Kan, Y., and Schuster, G. B. (1999) *Proc. Natl. Acad. Sci. U. S. A.* **96**, 8353–8358
11. Hall, D. B., Holmlind, R. E., and Barton, J. K. (1996) *Nature* **382**, 731–735
12. Saito, I., Nakamura, T., Nakatani, K., Yoshioka, Y., Yamaguchi, K., and Sugiyama, H. (1998) *J. Am. Chem. Soc.* **120**, 12686–12687
13. Steenken, S., and Jovanovic, S. V. (1997) *J. Am. Chem. Soc.* **119**, 617–618
14. Sugiyama, H., and Saito, I. (1996) *J. Am. Chem. Soc.* **118**, 7063–7068
15. Senthilkumar, K., Grozema, F. C., Guerra, C. F., Bickelhaupt, F. M., and Siebbeles, L. D. A. (2003) *J. Am. Chem. Soc.* **125**, 13658–13659
16. Cullis, P. M., Davis, A. S., Malone, M. E., Podmore, I. D., and Symons, M. C. R. (1992) *J. Chem. Soc. Perkins Trans. II*, 1409–1412
17. Sevilla, M. D., Becker, D., Yan, M., and Summerfield, S. R. (1991) *J. Phys. Chem.* **95**, 3409–3415
18. Bernhard, W. A. (1989) *J. Phys. Chem.* **93**, 2187–2189
19. Cullis, P. M., Evans, P., and Malone, M. E. (1996) *Chem. Commun.* 985–986
20. Gregoli, S., Olast, M., and Bertinchamps, A. (1982) *Radiat. Res.* **89**, 238–254
21. Milligan, J. R., Aguilera, J. A., and Ward, J. F. (1993) *Radiat. Res.* **133**, 151–157
22. Ito, T., Baker, S. C., Stickley, C. D., Peak, J. G., and Peak, M. J. (1993) *Int. J. Radiat. Biol.* **63**, 289–296
23. Purkayastha, S., Milligan, J. R., and Bernhard, W. A. (2007) *Radiat. Res.* **168**, 357–366
24. Purkayastha, S., and Bernhard, W. A. (2004) *J. Phys. Chem. B* **108**, 18377–18382
25. Steenken, S., Jovanovic, S. V., Bietti, M., and Bernhard, K. (2000) *J. Am. Chem. Soc.* **122**, 2373–2374
26. Doddridge, Z. A., Cullis, P. M., Jones, G. D. D., and Malone, M. E. (1998) *J. Am. Chem. Soc.* **120**, 10998–10999
27. Ding H., and Greenberg, M. M. (2007) *J. Am. Chem. Soc.* **129**, 772–773
28. Margolin, Y., Cloutier, J. F., Shafirovich, V., Geacintov, N. E., and Dedon, P. C. (2006) *Nat. Chem. Biol.* **2**, 365–366
29. Dedon, P. C. (2008) *Chem. Res. Toxicol.* **21**, 206–219
30. Putney, S. D., Benkovic, S. J., and Schimmel, P. R. (1981) *Proc. Natl. Acad. Sci. U. S. A.* **78**, 7350–7354
31. Greenberg, M. M., Weledji, Y. N., Kim, J., and Bales, B. C. (2004) *Biochemistry* **43**, 8178–8183
32. Kow, Y. W. (1989) *Biochemistry* **28**, 3280–3287
33. Price, M. A., and Tullius, T. D. (1992) *Methods Enzymol.* **212**, 194–219
34. Murata-Kamiya, N., Kamiya, H., Muraoka, M., Kaji, H., and Kasai, H. (1997) *J. Radiat. Res.* **38**, 121–131
35. Dedon, P. C., and Goldberg, I. H. (1992) *Chem. Res. Toxicol.* **5**, 311–332
36. Balasubramanian, B., Pogozelski, W. K., and Tullius, T. D. (1998) *Proc. Natl. Acad. Sci. U. S. A.* **95**, 9738–9743
37. Qian, S. Y., and Buettner, G. R. (1999) *Free Radic. Biol. Med.* **26**, 1447–1456
38. Yoshioka, Y., Kitagawa, Y., Takano, Y., Yamaguchi, K., Nakamura, T., and Saito, I. (1999) *J. Am. Chem. Soc.* **121**, 8712–8719
39. Spassky, A., and Angelov, D. (1997) *Biochemistry* **36**, 6571–6576
40. Haraguchi, K., Delaney, M. O., Wiederholt, C. J., Sambandam, A., Hantosi, Z., and Greenberg, M. M. (2002) *J. Am. Chem. Soc.* **124**, 3263–3269
41. Gasparutto, D., Ravanat, J.-L., Gerot, O., and Cadet, J. (1998) *J. Am. Chem. Soc.* **120**, 10283–10286
42. Tchou, J., Kasai, H., Shibutani, S., Chung, M. H., Laval, J., Grollman, A. P., and Nishimura, S. (1991) *Proc. Natl. Acad. Sci. U. S. A.* **88**, 4690–4694
43. Tretyakova, N. Y., Wishnok, J. S., and Tannenbaum, S. R. (2000) *Chem. Res. Toxicol.* **13**, 658–664
44. Tretyakova, N. Y., Burney, S., Pamir, B., Wishnok, J. S., Dedon, P. C., Wogan, G. N., and Tannenbaum, S. R. (2000) *Mutat. Res.* **447**, 287–303
45. Joffe, A., Geacintov, N. E., and Shafirovich, V. (2003) *Chem. Res. Toxicol.* **16**, 1528–1538
46. Ravanat, J. L., Saint-Pierre, C., and Cadet, J. (2003) *J. Am. Chem. Soc.* **125**, 2030–2031
47. Crean, C., Lee, Y. A., Yun, B. H., Geacintov, N. E., and Shafirovich, V. (2008) *ChemBioChem* **9**, 1985–1991
48. Pouget, J. P., Frelon, S., Ravanat, J. L., Testard, I., Odin, F., and Cadet, J. (2002) *Radiat. Res.* **157**, 589–595
49. Douki, T., Riviere, J., and Cadet, J. (2002) *Chem. Res. Toxicol.* **15**, 445–454
50. Paul, T., Young, M. J., Hill, I. E., and Ingold, K. U. (2000) *Biochemistry* **39**, 4129–4135
51. Rodriguez, H., Holmquist, G. P., D'Agostino, R., Jr., Keller, J., and Akman, S. A. (1997) *Cancer Res.* **57**, 2394–2403
52. Luo, G. M., Qi, D. H., Zheng, Y. G., Mu, Y., Yan, G. L., Yang, T. S., and Shen, J. C. (2001) *FEBS Lett.* **492**, 29–32
53. Rush, J. D., and Koppenol, W. H. (1986) *J. Biol. Chem.* **261**, 6730–6733
54. Wink, D. A., Nims, R. W., Saavedra, J. E., Utermahlen, W. E., Jr., and Ford, P. C. (1994) *Proc. Natl. Acad. Sci. U. S. A.* **91**, 6604–6608
55. Sawyer, D. T., Kang, C., Llobet, A., and Redman, C. (1993) *J. Am. Chem. Soc.* **115**, 5817–5818
56. Koppenol, W. H., and Liebman, J. F. (1984) *J. Phys. Chem.* **88**, 99–101
57. Reinke, L. A., Rau, J. M., and McCay, P. B. (1994) *Free Radic. Biol. Med.* **16**, 485–492
58. Welch, K. D., Davis, T. Z., and Aust, S. D. (2002) *Arch. Biochem. Biophys.* **397**, 360–369
59. Candeias, L. P., and Steenken, S. (2000) *Chemistry* **6**, 475–484
60. Cadet, J., Douki, T., and Ravanat, J. L. (2008) *Acc. Chem. Res.* **41**, 1075–1083
61. Misiasek, R., Crean, C., Joffe, A., Geacintov, N. E., and Shafirovich, V. (2004) *J. Biol. Chem.* **279**, 32106–32115
62. Giese, B., Amaudrut, J., Kohler, A.-K., Spormann, M., and Wessely, S. (2001) *Nature* **412**, 318–320
63. Kobayashi, K., and Tagawa, S. (2003) *J. Am. Chem. Soc.* **125**, 10213–10218
64. Shafirovich, V., and Geacintov, N. E. (2004) in *Long-Range Charge Transfer in DNA II* (Schuster, G. B., and Beratan, D., eds) pp. 129–157, Springer-Verlag, Berlin
65. Cadet, J., and Berger, M. (1985) *Int. J. Radiat. Biol. Relat. Stud. Phys. Chem. Med.* **47**, 127–143
66. Dizdaroglu, M., Dirksen, M. L., Simic, M. G., and Robbins, J. H. (1986) *Fed. Proc.* **45**, 1626
67. von Sonntag, C. (2006) *Free Radical-induced DNA Damage and Its Repair: A Chemical Perspective*, Springer-Verlag, Berlin
68. Douki, T., and Cadet, J. (1999) *Int. J. Rad. Biol.* **75**, 571–581
69. Kino, K., and Sugiyama, H. (2001) *Chem. Biol.* **8**, 369–378
70. Matter, B., Malejka-Giganti, D., Csallany, A. S., and Tretyakova, N. (2006) *Nucleic Acids Res.* **34**, 5449–5460
71. Leipold, M. D., Muller, J. G., Burrows, C. J., and David, S. S. (2000) *Biochemistry* **39**, 14984–14992
72. Cadet, J., Douki, T., Gasparutto, D., and Ravanat, J. L. (2003) *Mutat. Res.* **531**, 5–23
73. Cadet, J., Berger, M., Buchko, G. W., Joshi, P. C., Raoul, S., and Ravanat, J.-L. (1994) *J. Am. Chem. Soc.* **116**, 7403–7404
74. Dedon, P. C., and Tannenbaum, S. R. (2004) *Arch. Biochem. Biophys.* **423**, 12–22
75. Box, H. C. (2001) *Radiat. Res.* **155**, 634–636
76. Box, H. C., Dawidzik, J. B., Wallace, J. C., Hauer, C. R., Stack, R. F., Rajec, M. J., and Budzinski, E. E. (1999) *Radiat. Res.* **152**, 575–582
77. Packer, M. J., Dauncey, M. P., and Hunter, C. A. (2000) *J. Mol. Biol.* **295**, 85–103
78. Delaney, J. C., and Essigmann, J. M. (2008) *Chem. Res. Toxicol.* **21**, 232–252
79. McCulloch, S. D., and Kunkel, T. A. (2008) *Cell Res.* **18**, 148–161